

Barium- and strontium-enriched apatites in lamproites from West Kimberley, Western Australia

ALAN D. EDGAR

Department of Geology, University of Western Ontario, London, Ontario N6A 5B7, Canada

ABSTRACT

Apatites and fluorapatites with BaO up to 12.54 wt% and SrO up to 5.78 wt% occur in the lamproites from West Kimberley, Western Australia. These are the highest BaO values known for apatites in igneous rocks. Apatites with BaO > SrO occur in diopside leucite lamproites and to a lesser extent in olivine diopside leucite lamproites. Many apatites exhibit compositional zoning with decreasing BaO and increasing SrO from core to rim. Phlogopite leucite lamproites have SrO > BaO. Sr-rich apatites almost invariably have significantly higher F values than Ba-rich varieties. Cl is absent or very low in both varieties of apatites. All apatites have decreasing Ba + Sr with increasing Ca (as atoms per formula unit). Whether a Ba- or Sr-enriched apatite crystallizes appears to be related to the Ba and Sr enrichment in the magma from which each rock crystallized and on the stage of crystallization of the magma. Micas and amphiboles coexisting with these apatites are not appreciably enriched in either Ba or Sr.

INTRODUCTION

A survey of the literature (e.g., Nash, 1984) indicates that analyzing for BaO and, to a lesser extent, SrO in naturally occurring apatites in igneous rocks is uncommon. An extremely Ba-enriched apatite, named alforsite, was described from metaevaporites in Fresno and Mariposa Counties, California, by Newberry et al. (1981) who gave two analyses: $(\text{Ba}_{4.6}\text{Sr}_{0.19}\text{Ca}_{0.13})(\text{P}_{2.98}\text{Si}_{0.01})\text{O}_{11.96}\text{Cl}_{0.90}\text{F}_{0.05}$ and $(\text{Ba}_{4.05}\text{Ca}_{0.75}\text{Sr}_{0.24}\text{Pb}_{0.03})(\text{P}_{2.94}\text{Si}_{0.01})\text{O}_{11.93}\text{Cl}_{0.93}\text{F}_{0.14}$, corresponding to 67.7 wt% BaO and 2.7 wt% SrO, respectively. In this mineral, Cl greatly exceeds F, with Cl being 3.5–3.6 wt% and F up to 0.7 wt%. Apatites with high SrO values, termed saamites, were reported by Elfimov et al. (1962) in alkalic pegmatites cutting dunites in Inagil massif, Southern Yukatita. Their analyses gave 46.1 wt% SrO, 2.7 wt% BaO, and 1.7 wt% F. For predominantly Ca-bearing apatites in mantle-derived igneous rocks and their xenoliths, Dawson et al. (1985) found BaO and SrO present only in minor amounts, ranging from 0.30 to 1.25 wt%. Analyses of SrO from apatites in minettes and their xenoliths range from 0.01 to 0.88 wt% (Jones and Smith, 1983). Data for BaO and SrO in apatites in lamproites are sparse. Kuehner et al. (1981) reported a maximum BaO of 0.19 wt% in four apatites from Leucite Hills, Wyoming whereas SrO in apatites from the same locality has a maximum value of 0.46 wt% (Carmichael, 1967).

This paper describes apatites in various lamproites from the Fitzroy Basin, West Kimberley, Western Australia (Jacques et al., 1984; Prider, 1960) with extremely high Ba contents (BaO up to 12.2 wt%) and moderately high Sr values (SrO up to 5.8 wt%) relative to those of other apatites in igneous rocks. Although the majority of apa-

tites in the lamproites from this area contain <1 wt% BaO and <2 wt% SrO, apatite from a diopside leucite lamproite (WK18) from Wolgidee Hills (Prider, 1960) is characterized by very high Ba contents. High but less extreme Ba enrichment is also found in apatites from an olivine diopside leucite lamproite (WK25) from Mitchell's Pyramid (Prider, 1960) and from a second diopside leucite lamproite (WK17) from Wolgidee Hills. Samples of apatites from phlogopite leucite lamproites (WK5 from 81-mile vent; WK10 and WK13 from Mt. North) are enriched in Sr.

The BaO and SrO contents in the West Kimberley apatites are much greater than for apatites from a number of other lamproites (Edgar, unpublished data). These include apatites from Gausberg, Antarctica (Sheraton and Cundari, 1980), Smoky Butte, Montana (Mitchell et al., 1987), and Prairie Creek, Arkansas (Scott-Smith and Skinner, 1984).

The cationic and anionic substitutions in the apatite structure have been extensively studied in synthetic apatites (Roy et al., 1978). Moore (1982, 1984) has reviewed the complex crystal structure of phosphate minerals, including apatite. Roy et al. (1978) proposed the general formula $\text{A}_{10}(\text{MO}_4)_6\text{X}_2$. In the apatite structure, both Ba and Sr replace Ca in the A site and F substitutes for O, OH, and Cl in the X site. Complete substitutions of Ca by Ba and Ca by Sr are known in synthetic apatites (Simpson, 1968). Substitution of a larger cation such as ^{16}Ba ($r = 1.36 \text{ \AA}$; Shannon, 1976) for ^{16}Ca ($r = 1.00 \text{ \AA}$) in the A site produces an increase in the cell parameters of apatite. On the basis of the few available analyses of BaO and SrO in apatites in igneous rocks (Nash, 1984), substitution by both Ba and Sr for Ca appears to be limited. This may reflect either (1) the normally very small

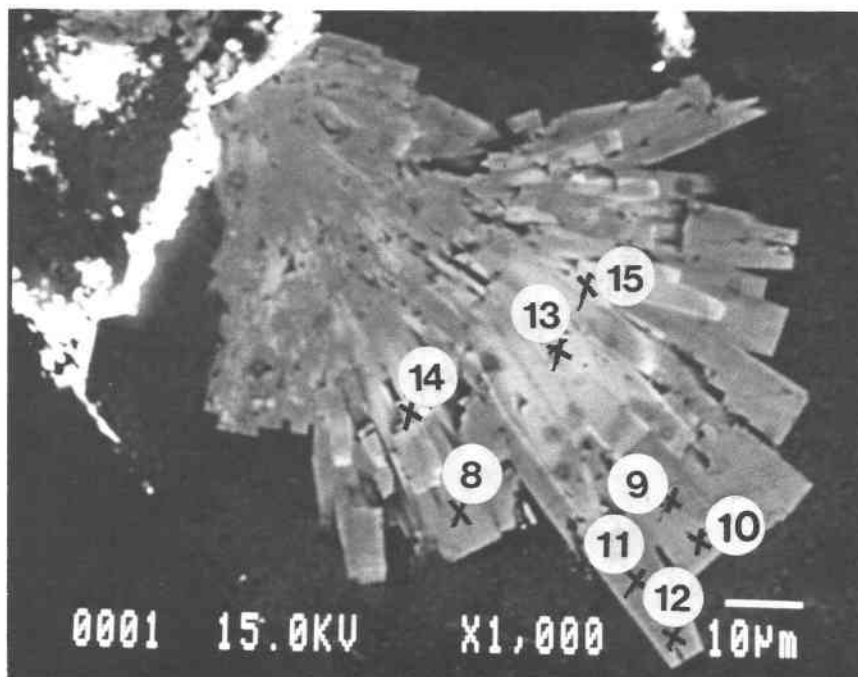


Fig. 1. Backscattered-electron image of sheaflike apatite aggregates in diopside leucite lamproite (WK18). Lighter areas of photograph represent more Ba- and Sr-enriched apatites. Numbers correspond to analyses given in Table 1.

amounts of Ba and Sr relative to Ca in the magmas from which such apatite crystallizes or (2) the substitutions being more complex.

PETROGRAPHY

Apatite is a common accessory groundmass mineral in most lamproites. According to the nomenclature proposed by Jacques et al. (1984) for the West Kimberley lamproites, the samples with high-Ba and high-Sr apatites discussed here are transitional rocks with mineral assemblages intermediate between olivine and leucite lamproites. Detailed petrographic descriptions of these rocks are given by Prider (1960) and Jacques et al. (1984).

In one of the diopside leucite lamproites (WK18), apatite occurs as sheaflike aggregates, either in the form of double or single sheaves; as euhedral stubby prisms; or as rare individual laths. The sheaflike habits are most readily observed on backscattered-electron photographs taken on the JEOL 8600 electron microprobe used in this study. Individual apatite grains may be as long as 10 μm and 4–5 μm across. In the same rock, well-developed single sheaves of apatite also occur (Fig. 1) with grains as long as 80 μm and 10–12 μm across.

These spectacular, although tiny, aggregates of apatite appear to be restricted to WK18. They were not observed in the other diopside leucite lamproite (WK17) where apatite occurs as very small (>5 μm), subhedral to anhedral grains and as laths. In the olivine diopside leucite lamproite (WK25), in the phlogopite leucite lamproites (WK5, WK10, WK13), and in the diopside potassic rich-

terite leucite lamproite (WK22), apatites are present as small stubby prisms, some with apparent optical zoning. Although small, these grains are occasionally large enough to permit core and rim analysis.

ANALYTICAL METHODS

All samples were analyzed on a JEOL 8600 model Superprobe using an accelerating voltage of 15 kV, a 1- μm -diameter beam, and a beam current of 10 nA. All analyses were done using a fluorapatite standard from Durango, Mexico (U.S. National Museum 104021). Ba and Sr were standardized using pure BaSO₄ and SrTiO₃, respectively. Frequent analyses of these standards gave excellent results and assured the quality of the analyses of the apatites.

The JEOL 8600 microprobe was fitted with a backscattered-electron detector allowing observations of very fine grained textures (Fig. 1) and analyses of small grains observed under high magnifications. This technique was also used to ascertain that none of the apatites analyzed contained inclusions of Ba- or Sr-bearing minerals.

RESULTS

Representative analyses of apatites with >1 wt% BaO and/or >2 wt% SrO are given in Table 1, and Ba + Sr is plotted against Ca in Figure 2. Using the general formula A₁₀(MO₄)₆X₂ (Roy et al., 1978), the number of atoms in the structural formula may be calculated on the basis of the analyzed cations per 24 oxygens, or the analyzed cations may be normalized to 10 (Ca + Ba + Sr + Mg +

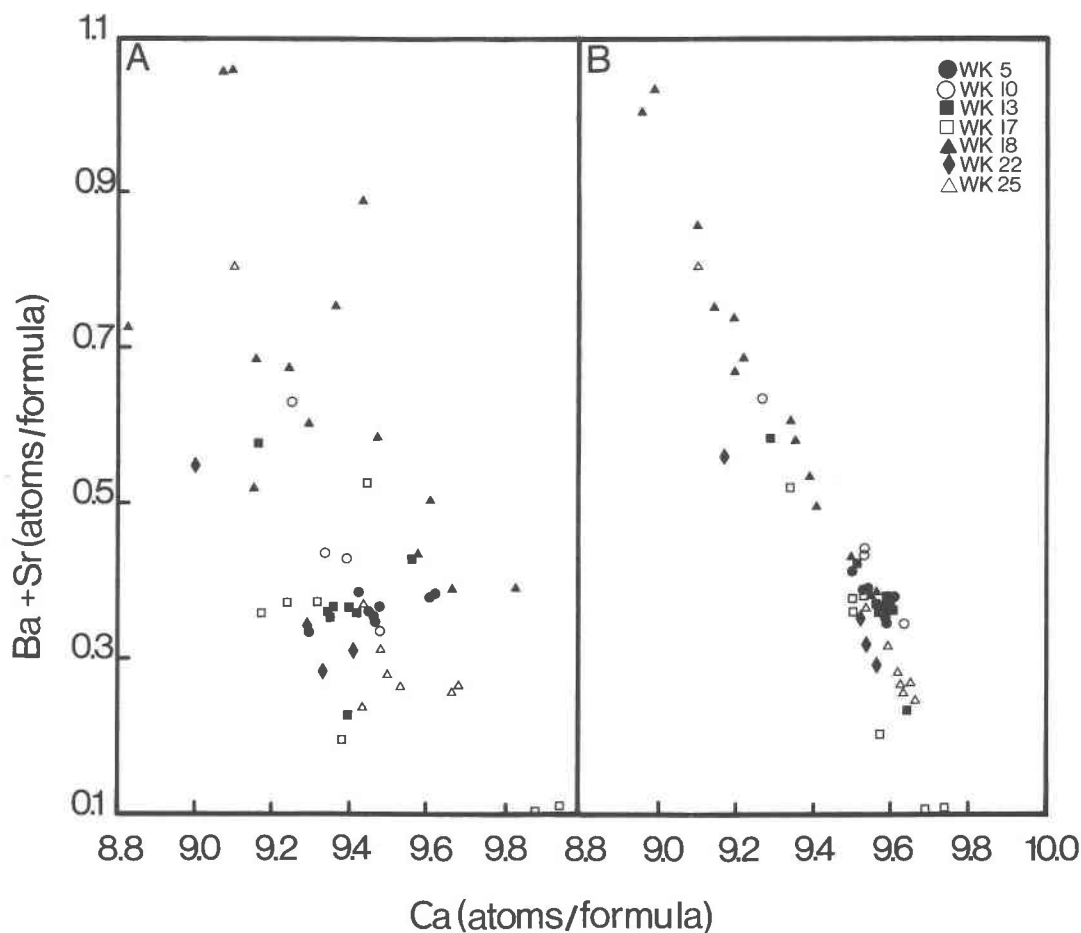


Fig. 2. Ca vs. Ba + Sr in apatites from lamproites WK17, WK22, WK18, WK13, WK5, WK10, and WK25: (A) as cations per 24 oxygens; (B) as cations per formula unit normalized to 10 atoms (Ca + Ba + Sr + Mg + Na + K + Fe) in the A site.

Na + K + Fe = 10) in the A site and to 6 (P + Si + Al + Ti = 6) in the M site. The latter process, however, does not account for different charges in these cations and results in the total oxygen atoms differing from the 24 implied by the formula. Of more significance is the fact that neither method of representing the structural formula takes into account the possible substitutions and partial substitutions of atoms that are not determined in the analysis. Consideration of the very large number of atoms involved and the complexity of the substitutions is beyond the scope of the present study but is stressed by Roy et al. (1978, see particularly p. 190 and following) and by Moore (1982, 1984). Because of these difficulties, many authors (e.g., Nash, 1984; Newberry et al., 1981; Prins, 1973) give no structural formula for apatite analyses.

Rare-earth elements (REEs) and C are the most likely substitutions in the A and M sites, respectively. Semi-quantitative analyses for REEs in a few samples yielded values of 1.4–1.7 wt% total REE oxides. C could not be analyzed in the present study. The complex substitutions and partial substitutions in apatites result in structural formulas, calculated on the basis of 24 oxygens (Table 1),

appearing to be deficient or to have excess atoms in both their A and M sites. The possible effects of substitution or partial substitution by unanalyzed elements for Ca, Ba, and Sr is indicated by the spread of points in the Ca vs. Ba + Sr plot (Fig. 2A) relative to the more linear relationship of increasing Ba + Sr with decreasing Ca (Fig. 2B) when cations in the A site are normalized to 10.

The possibility of Cl substituting for F in these apatites was examined by analyzing selected samples for Cl. The maximum Cl found is 0.04 wt%, and in most apatites it cannot be detected.

The data in Table 1 and Figure 2 show a large spread in the BaO and SrO contents of apatites both between and within individual lamproites. In samples WK5, WK10, and WK13 (phlogopite leucite lamproites), apatites are noticeably Sr enriched, with SrO contents between about 2.00 and 5.78 wt%, and their BaO contents are <1.0 wt%. In the olivine diopside leucite lamproite (WK25), most apatites analyzed have <1.0 wt% BaO and SrO > BaO except one exceptionally Ba-rich grain with 9.78 wt% BaO and 1.38 wt% SrO in its core and 2.55 wt% BaO and 0.75 wt% SrO in its rim (Table 1, WK25,

TABLE 1. Representative analyses of apatites from West Kimberley lamproites

	Phlogopite leucite lamproite (WK5)						Phlogopite leucite lamproite (WK10)			Phlogopite leucite lamproite (WK13)				
	3	4(C)	5(I)	6(R)	7(C)	8(R)	2	4	5	3(C)	4(R)	7	8(C)	9(R)
SiO ₂	0.10	0.00	0.00	0.02	0.00	0.00	0.00	0.09	0.14	0.15	0.16	0.25	0.04	0.14
TiO ₂	0.08	0.15	0.14	0.10	0.05	0.08	0.20	0.06	0.10	0.04	0.06	0.05	0.07	0.04
Al ₂ O ₃	0.00	0.00	0.00	0.00	0.00	0.00	0.00	0.00	0.00	0.03	0.02	0.00	0.00	0.03
FeO	0.17	0.26	0.28	0.22	0.16	0.11	0.34	0.10	0.21	0.06	0.10	0.26	0.09	0.12
MgO	0.07	0.03	0.04	0.05	0.03	0.04	0.02	0.05	0.02	0.11	0.10	0.08	0.15	0.12
CaO	52.42	53.31	52.51	52.78	53.79	53.58	50.79	52.13	51.47	52.73	53.25	50.75	53.57	53.89
Na ₂ O	0.00	0.00	0.00	0.00	0.00	0.00	0.00	0.00	0.00	0.00	0.00	0.00	0.00	0.00
K ₂ O	0.09	0.17	0.18	0.20	0.05	0.05	0.18	0.02	0.03	0.11	0.15	0.30	0.07	0.10
P ₂ O ₅	40.78	40.01	38.51	38.60	40.76	40.30	38.85	39.30	39.08	40.56	40.34	39.42	40.71	39.69
BaO	0.49	0.39	0.49	0.39	0.49	0.40	0.96	0.49	0.61	0.32	0.42	0.73	0.44	0.57
SrO	3.25	3.89	3.55	3.62	3.52	3.54	5.78	3.08	3.98	3.44	3.37	5.35	3.50	4.04
F	1.56	3.03	2.37	1.92	1.02	0.81	1.67	5.87	4.93	5.40	2.79	4.31	2.79	2.16
Total (less O = F)	98.35	97.73	100.23	97.25	97.47	99.45	98.10	98.73	98.51	99.99	99.59	99.69	100.25	98.99
Ca	9.292	9.459	9.604	9.623	9.448	9.479	9.249	9.476	9.399	9.338	9.420	9.160	9.405	9.566
Ba	0.030	0.030	0.031	0.031	0.030	0.030	0.061	0.031	0.041	0.020	0.030	0.051	0.030	0.040
Sr	0.308	0.328	0.349	0.358	0.335	0.337	0.572	0.306	0.389	0.338	0.328	0.526	0.335	0.388
K	0.020	0.040	0.042	0.040	0.020	0.020	0.041	0.000	0.000	0.020	0.040	0.061	0.020	0.020
Na	0.000	0.000	0.000	0.000	0.000	0.000	0.000	0.000	0.000	0.000	0.000	0.000	0.000	0.000
Fe	0.020	0.040	0.041	0.031	0.020	0.020	0.051	0.010	0.030	0.010	0.010	0.040	0.010	0.020
Mg	0.020	0.010	0.010	0.010	0.000	0.010	0.000	0.010	0.000	0.030	0.020	0.020	0.039	0.030
P	5.704	5.610	5.562	5.563	5.655	5.638	5.594	5.651	5.631	5.682	5.638	5.628	5.653	5.554
Si	0.020	0.000	0.000	0.000	0.000	0.000	0.000	0.010	0.020	0.020	0.030	0.040	0.010	0.020
Ti	0.010	0.020	0.021	0.010	0.011	0.010	0.031	0.010	0.010	0.010	0.010	0.010	0.010	0.010
Al	0.000	0.000	0.000	0.000	0.000	0.000	0.000	0.000	0.000	0.000	0.000	0.000	0.000	0.000
F	0.815	1.591	1.272	1.043	0.532	0.417	0.449	3.142	2.662	1.411	1.449	2.288	1.438	1.135

Note: C = core, I = intermediate, R = rim. Samples listed under only a number (i.e., without the C, I, or R designation) were too small to analyze in different spots.

analyses 8 and 9). The apatites in WK17 (diopside leucite lamproite) are generally Ba-rich varieties although three samples (Table 1, WK17, analyses 5, 7, and 9) have SrO > BaO. With a single exception, apatites in the other diopside leucite lamproite (WK18) are extremely enriched in Ba, with BaO values up to 12.54 wt% (Table 1, WK18, analysis 13). The highest BaO in the apatites in WK18 occurs in the single sheaflike aggregates (Fig. 1).

Variation in Ba and Sr in apatite from the same rock is caused, in part, by compositional zoning as indicated by core to rim analyses (Table 1). In the extremely Ba-enriched apatites from WK18, SrO increases markedly and BaO decreases only slightly from core to rim with a corresponding decrease in CaO (Table 1, WK18, analyses 9, 10, 11, and 12). The apatites in WK18 show decreasing BaO/SrO and CaO/SrO and increasing CaO/BaO from cores to rims. In one of the Ba-enriched apatites in WK25 (Table 1, WK25, analyses 8 and 9) both SrO and BaO decrease as CaO increases from core to rim, resulting in an overall decrease in BaO/SrO and increase in CaO/BaO and CaO/SrO from core to rim. Similarly, in the Sr-enriched apatites in WK10, both BaO and SrO decrease and CaO increases from core to rim (Table 1, WK10, analyses 2 and 4), resulting in a slight decrease in BaO/SrO and increase in CaO/BaO and CaO/SrO from core to rim.

Compositional zoning in apatites in WK18 with respect to BaO and SrO can be easily detected on the back-scattered-electron photograph (Fig. 1) in which the lighter

areas represent zones with higher mean atomic number (higher Ba and Sr). In Figure 1 the spots analyzed are numbered according to the analysis number given in Table 1. Spots 13, 14, and 15 (Fig. 1) have higher BaO (>10 wt%) and slightly higher SrO values than the low BaO (<4 wt%) and lower SrO values for the darker areas.

Many of the apatites in the West Kimberley lamproites are fluorapatites. Although the amount of F is very variable (Table 1), the Ba-enriched apatites are characterized by lower F contents (e.g., WK18—0.00 to 1.07 wt% F) than those in the Sr-enriched varieties (e.g., WK13—2.16 to 5.40 wt% F, WK10—1.67 to 5.87 wt% F). Compositional zoning with respect to F is also present. In the Ba-enriched apatites in WK18, there is a decrease in CaO/F, BaO/F, and SrO/F, whereas in Sr-enriched apatites (e.g., WK25), CaO/F increases only slightly.

DISCUSSION

The apatites from the lamproites of the West Kimberley region have the highest Ba values recorded for apatites found in igneous rocks. Sr contents are also very high in these apatites. The high Ba and Sr may reflect the high Ba and Sr found in the lamproite magmas of this area. Lamproites are considered to represent pristine, mantle-derived magmas in which little differentiation has occurred (Bergman, 1987). Therefore, any early-crystallizing minerals with structures capable of incorporating Ba and Sr might be expected to reflect high Ba and Sr values

TABLE 1.—Continued

	Diopside leucite lamproite (WK17)					Diopside leucite lamproite (WK18)							
	2	5	6	7	9	4	5	6	8	9	10	11(C)	12(R)
SiO ₂	0.43	0.54	0.00	0.42	0.75	0.42	0.00	0.86	0.00	0.00	0.00	0.00	0.00
TiO ₂	0.33	0.13	0.27	0.13	0.06	0.51	0.19	0.56	0.23	0.18	0.17	0.22	0.23
Al ₂ O ₃	0.03	0.05	0.01	0.03	0.02	0.08	0.00	0.01	0.00	0.00	0.00	0.00	0.00
FeO	0.37	0.31	0.27	0.25	0.23	0.30	0.38	0.19	0.35	0.29	0.35	0.35	0.55
MgO	0.10	0.07	0.00	0.04	0.08	0.00	0.00	0.00	0.00	0.00	0.00	0.00	0.00
CaO	53.10	53.59	52.19	51.49	51.62	48.98	51.41	51.12	51.51	54.73	50.85	54.94	53.38
Na ₂ O	0.24	0.03	0.25	0.07	0.09	0.00	0.00	0.00	0.00	0.00	0.00	0.00	0.00
K ₂ O	0.27	0.16	0.12	0.12	0.14	0.30	0.34	0.21	0.10	0.05	0.12	0.11	0.14
P ₂ O ₅	40.30	40.73	38.90	39.97	40.23	39.59	39.30	39.21	38.04	39.78	38.00	38.95	38.68
BaO	2.59	0.86	3.21	0.88	0.69	5.56	2.12	6.25	4.04	2.91	2.59	3.46	3.24
SrO	0.28	3.29	3.19	3.22	3.08	3.72	5.51	1.14	3.22	2.04	5.76	1.68	2.96
F	0.87	1.74	0.65	2.15	2.42	0.23	1.07	0.00	0.57	0.42	0.76	0.10	0.58
Total (less O = F)	98.59	100.78	98.79	97.86	98.40	99.59	99.87	99.55	97.83	100.24	98.57	99.77	99.53
Ca	9.376	9.315	9.436	9.242	9.173	8.818	9.239	9.148	9.468	9.663	9.359	9.825	9.612
Ba	0.168	0.059	0.213	0.060	0.056	0.364	0.141	0.412	0.268	0.188	0.175	0.229	0.212
Sr	0.030	0.312	0.314	0.312	0.299	0.364	0.534	0.110	0.320	0.198	0.578	0.160	0.293
K	0.059	0.039	0.020	0.020	0.040	0.061	0.081	0.040	0.021	0.020	0.021	0.020	0.020
Na	0.079	0.020	0.081	0.020	0.040	0.000	0.000	0.000	0.000	0.000	0.000	0.000	0.000
Fe	0.050	0.039	0.041	0.030	0.030	0.040	0.050	0.030	0.052	0.040	0.052	0.050	0.081
Mg	0.030	0.020	0.000	0.010	0.020	0.000	0.000	0.000	0.000	0.000	0.000	0.000	0.000
P	5.624	5.593	5.554	5.658	5.644	5.636	5.481	5.543	5.528	5.545	5.531	5.466	5.493
Si	0.069	0.175	0.000	0.070	0.136	0.071	0.000	0.281	0.000	0.000	0.000	0.000	0.000
Ti	0.040	0.039	0.030	0.020	0.010	0.061	0.040	0.141	0.031	0.020	0.000	0.030	0.030
Al	0.000	0.020	0.000	0.000	0.000	0.020	0.000	0.000	0.000	0.000	0.000	0.000	0.000
F	0.456	0.897	0.340	1.148	1.276	0.121	0.564	0.000	0.308	0.109	0.413	0.060	0.303

TABLE 1.—Continued

	Diopside leucite lamproite (WK18)			Diopside K-richterite leucite lamproite (WK22)			Olivine diopside leucite lamproite (WK25)					
	13	14	15	5	6	7	3(C)	4(R)	6	7	8(C)	9(R)
SiO ₂	0.00	0.01	0.05	0.44	0.41	0.49	0.00	0.00	0.00	0.00	0.00	0.00
TiO ₂	0.77	0.68	0.69	0.16	0.23	0.22	0.09	0.11	0.09	0.10	0.58	0.17
Al ₂ O ₃	0.00	0.04	0.00	0.13	0.11	0.03	0.00	0.00	0.00	0.00	0.04	0.00
FeO	0.27	0.24	0.33	0.22	0.43	0.37	0.30	0.28	0.36	0.33	0.35	0.38
MgO	0.00	0.00	0.00	0.14	0.10	0.12	0.05	0.02	0.01	0.04	0.00	0.00
CaO	48.31	49.88	48.05	52.96	50.12	53.49	54.25	53.68	55.03	54.89	48.93	53.35
Na ₂ O	0.00	0.00	0.00	0.14	0.40	0.09	0.00	0.00	0.00	0.00	0.00	0.00
K ₂ O	0.07	0.07	0.11	0.11	0.25	0.21	0.23	0.27	0.26	0.20	0.18	0.18
P ₂ O ₅	36.61	35.73	36.50	40.69	39.64	40.02	40.93	40.56	40.26	41.36	37.78	40.80
BaO	12.54	10.40	12.20	0.51	1.14	0.57	0.61	0.61	0.58	0.50	9.78	2.55
SrO	1.74	1.69	2.07	3.28	4.94	2.91	2.88	3.41	2.38	2.71	1.38	0.75
F	0.00	0.31	0.00	1.93	1.65	1.59	2.95	2.64	1.68	2.67	0.85	0.31
Total (less O = F)	100.31	98.92	100.01	99.90	98.73	99.42	101.05	100.47	99.93	101.70	99.50	98.35
Ca	9.099	9.428	9.069	9.289	9.000	9.403	9.480	9.440	9.677	9.501	9.100	9.428
Ba	0.877	0.721	0.846	0.030	0.070	0.039	0.039	0.039	0.039	0.029	0.668	0.169
Sr	0.180	0.170	0.212	0.315	0.483	0.276	0.275	0.326	0.227	0.252	0.136	0.069
K	0.011	0.011	0.010	0.020	0.060	0.039	0.039	0.059	0.060	0.039	0.042	0.040
Na	0.000	0.000	0.000	0.039	0.121	0.020	0.000	0.000	0.000	0.000	0.000	0.000
Fe	0.000	0.032	0.053	0.030	0.060	0.049	0.039	0.039	0.049	0.049	0.052	0.050
Mg	0.000	0.000	0.000	0.030	0.020	0.030	0.010	0.000	0.000	0.010	0.000	0.000
P	5.453	5.345	5.439	5.628	5.617	5.559	5.647	5.642	5.583	5.648	5.551	5.690
Si	0.000	0.000	0.021	0.069	0.070	0.079	0.000	0.000	0.000	0.000	0.000	0.000
Ti	0.115	0.095	0.095	0.020	0.030	0.030	0.010	0.010	0.010	0.010	0.073	0.020
Al	0.000	0.000	0.000	0.020	0.020	0.000	0.000	0.000	0.000	0.000	0.000	0.000
F	0.000	0.170	0.000	1.004	0.866	0.830	1.529	1.361	0.868	1.359	0.459	0.159

in the parental magma. Although no adequate discussion of partitioning between mineral phases and magma can be made in the absence of trace-element data for all phases, some quantitative approximations are useful. For the West Kimberley lamproites, in which average Ba values (11100 ppm) are higher than those for any other lamproites (Bergman, 1987), the principal early-formed minerals likely to contain Ba and Sr are phlogopite and richterite that occur as phenocrysts and microphenocrysts. Analyses of BaO in these phases (Edgar, unpublished data) do not indicate any exceptionally high values (BaO < 1.0 wt% in phlogopite and < 0.2 wt% in amphibole). SrO has not been determined, and neither BaO nor SrO is available for leucite or K-feldspar in these rocks.

The apatites in the West Kimberley rocks show no textural evidence of there necessarily being early-crystallizing minerals; the apatites usually occur as groundmass phases. However, the sheaflike masses of apatite found in WK18 (Fig. 1) are reminiscent of quench textures. This similarity suggests that these highly Ba-enriched apatites formed directly from a liquid during rapid consolidation of the lamproite magma.

The degree of enrichment of Ba and Sr in these apatites may be compared to Ba and Sr contents of the same rock types using the data of Jacques et al. (1984). The most Ba-enriched apatites occur in a diopside leucite lamproite (WK18) and two apatites from the olivine diopside leucite lamproite (WK25) (Table 1). The other diopside leucite lamproite (WK17) also has some moderately high Ba apatites. The remaining rocks (WK5, WK10, WK13—phlogopite leucite lamproites, WK22—diopside potassic richterite leucite lamproite) contain apatites that are predominantly Sr enriched. For olivine diopside leucite lamproite (sample WK25 of this study), Jacques et al. (1984, Table 5, analysis 10) found 31466 ppm Ba and 1070 ppm Sr in their whole-rock analyses. This Ba value is three orders of magnitude greater than that of 20 other West Kimberley lamproites (Jacques et al., 1984, Table 5). For diopside leucite lamproites (samples WK17, WK18 in this study), Jacques et al. (1984, Table 5, analysis 13) found 13939 ppm Ba and 985 ppm Sr in the whole-rock analysis. This Ba value is greater than the average Ba content of lamproites from West Kimberley (Bergman, 1987) and may account for the high-Ba apatites found in these rocks. In contrast, the Sr-rich apatites found in WK5, WK10, and WK13 are from phlogopite leucite lamproites. For this type of lamproite, Jacques et al. (1984, Table 5, analysis 8) determined lower Ba (10377 ppm) and higher Sr (1990 ppm) than in the other lamproites cited above. These comparisons suggest that the Ba and Sr enrichment in apatites is controlled by the Ba and Sr contents of the host magmas.

The spread in the Ca, Ba, and Sr contents in apatites (Fig. 2a) may result not only from compositional zoning and complex substitutions but also from the stage at which the apatite crystallized and from the available F in the magma. Table 1 indicates that Ba-enriched apatites have very low F contents relative to Sr-enriched ones (compare

WK18 and WK10, Table 1). The availability of F depends on the precrystallization or cocrystallization of other F-bearing phases such as phlogopite and richterite. Thus, the high-F apatites tend to occur in the phlogopite- and richterite-bearing lamproites rather than in lamproites in which mica and amphibole are rare.

ACKNOWLEDGMENTS

The samples used in this study were collected by Dr. Makoto Arima of Yokohama National University. Technical assistance from R. L. Barnett, D. Kingston, D. M. Forsyth, H. E. Charbonneau, and J. Forth is gratefully acknowledged. I thank the Natural Science and Engineering Research Council of Canada for operating and major installation grants.

REFERENCES CITED

- Bergman, S.C. (1987) Lamproites and other potassium-rich rocks: A review of their occurrences, mineralogy, and geochemistry. In J.G. Fitton and B.G.J. Upton, Eds., *Alkaline igneous rocks*, p. 103–190. Blackwell, London.
- Carmichael, I.S.E. (1967) The mineralogy and petrology of the volcanic rocks from the Leucite Hills, Wyoming. *Contributions to Mineralogy and Petrology*, 15, 24–66.
- Dawson, J.B., Smith, J.V., and Jones, A.P. (1985) A comparative study of bulk rock and mineral chemistry of olivine melilitites and associated rocks from east and South Africa. *Neues Jahrbuch für Mineralogie Abhandlungen*, 152, 143–175.
- Elfimov, A.S., Kravchenko, S.M., and Vasih'eva, Z.V. (1962) Strontium apatite: A new mineral. *Akademiya Nauk SSSR Doklady*, 142, 439–442.
- Jacques, A.L., Lewis, J.D., Smith, C.B., Gregory, G.P., Ferguson, J., Chappell, B.W., and McCulloch, M.T. (1984) The diamond-bearing ultrapotassic (lamproitic) rocks of the West Kimberley region, Western Australia. In J. Kornprobst, Ed., *Proceedings of the Third International Kimberlite Conference*, Vol. 1—Kimberlites and related rocks, 9, 225–255. Elsevier, Amsterdam.
- Jones, A.P., and Smith, J.V. (1983) Petrological significance of mineral chemistry in the Agatha Peak and the Thumb minettes, Navajo volcanic field. *Journal of Geology*, 91, 643–656.
- Kuehner, S.M., Edgar, A.D., and Arima, M. (1981) Petrogenesis of the ultrapotassic rocks from the Leucite Hills, Wyoming. *American Mineralogist*, 66, 663–677.
- Mitchell, R.H., Platt, R.G., and Downey, M. (1987) Petrology of lamproites from Smokey Butte, Montana. *Journal of Petrology*, 28, 645–678.
- Moore, P.B. (1982) Pegmatite minerals of P(V) and B(II). *Mineralogical Association of Canada Short Course Handbook*, 8, 267–291.
- (1984) Crystallochemical aspects of the phosphate minerals. In J.O. Nriagu and P.B. Moore, Eds., *Phosphate minerals*, p. 156–170. Springer-Verlag, New York.
- Nash, W.P. (1984) Phosphate minerals in terrestrial igneous and metamorphic rocks. In J.O. Nriagu and P.B. Moore, Eds., *Phosphate minerals*, p. 215–241. Springer-Verlag, New York.
- Newberry, N.G., Essene, E.J., and Peacor, D.R. (1981) Alforsite, a new member of the apatite group: The barium analogue of chloroapatite. *American Mineralogist*, 66, 1050–1053.
- Prider, R.T. (1960) The leucite lamproite of the Fitzroy Basin, Western Australia. *Journal of the Geological Society of Australia*, 6, 71–118.
- Prins, P. (1973) Apatite from African carbonatites. *Lithos*, 6, 133–144.
- Roy, D.M., Drafall, L.E., and Roy, R. (1978) Crystal chemistry, crystal growth, and phase equilibria of apatites. In A.M. Alper, Ed., *Phase diagrams, material sciences, and technology*, 6-V, 186–239. Academic Press, New York.
- Scott-Smith, B.H., and Skinner, E.M.W. (1984) A new look at Prairie Creek, Arkansas. In J. Kornprobst, Ed., *Proceeding of the Third International Kimberlite Conference*, Vol. 1—Kimberlites and related rocks, 9, 255–284. Elsevier, Amsterdam.

Shannon, R.D. (1976) Revised effective ionic radii and systematic studies of interatomic distances in halides and chalcogenides. *Acta Crystallographica*, A32, 751-767.

Sheraton, J.W., and Cundari, A. (1980) Leucitites from Gaussberg, Antarctica. *Contributions to Mineralogy and Petrology*, 71, 417-427.

Simpson, D.R. (1968) Substitutions in apatite: In potassium-bearing apatite. *American Mineralogist*, 53, 432-444.

MANUSCRIPT RECEIVED AUGUST 26, 1988

MANUSCRIPT ACCEPTED MARCH 6, 1989